Preferred citation: J. Kananen, H. Rajatora and K. Niskanen. Reversible Compression of Sheet Structure. In **The science of papermaking**, *Trans. of the XIIth Fund. Res. Symp. Oxford, 2001*, (C.F. Baker, ed.), pp 1043–1066, FRC, Manchester, 2018. DOI: 10.15376/frc.2001.2.1043.

REVERSIBLE COMPRESSION OF SHEET STRUCTURE

Juha Kananen, Hanna Rajatora and Kaarlo Niskanen

KCL Science and Consulting
P.O. Box 70, 02151 Espoo, Finland
juha.kananen@kcl.fi

ABSTRACT

We study the compression behavior in the thickness direction of paper using quasi-static pressure cycles from 0–10 MPa. The reversible component of compression agreed reasonably well with the following equation:

$$\varepsilon = \phi^* \cdot \left[1 - \exp\left(-\frac{p}{E^*}\right)\right]$$

where ϕ^* is the volume fraction (porosity) of compressible pores, and E^* is the effective elastic modulus characterizing the compression of the pores. The model can be derived both from the height distribution of pore space and from the general linear relationship between logarithmic strain and pressure. In handsheets, the fitted porosity parameter ϕ^* ranged from 0.13–0.22 depending on sheet density. The values of the elastic modulus E^* varied between 4 and 5 MPa. They could even be set constant at ca. 4.5 MPa without a significant loss of model agreement. Our results suggest that the reversible compression behavior of paper depends primarily on the porosity of the fiber network and only a little on the furnish composition.

INTRODUCTION

We study how paper structure and furnish composition influences the z-directional compression behavior of dry paper. The compression of paper and board is important in calendering, printing, die-cutting and scoring, etc. These operations induce a compression of paper structure that is partly reversible (at some rate) and partly irreversible. The net result on paper properties depends on the relative proportions of the reversible and irreversible compression.

The target of calendering is to permanently reduce surface roughness without losing porosity in the middle layers of the sheet. In the ideal case the calendering nips induce permanent compression in the surface layers of the paper and reversible compression in the other layers. The first calendering nip seems to have the largest effect on paper structure. Ivarsson [1] observed that the largest loss of paper thickness tends to occur when paper is compressed for the first time. Additional compressions cause primarily reversible compression. Schaffrath and Göttsching [2,3] found that the surface layers of paper compress irreversibly more than the middle layers in the first compression. Obviously the irreversible compression in surface layers is sensitive to the starting level of roughness. For optimal calendering results the properties of the middle layers should be such that they recover elastically from compression.

The coupling between the surface and bulk compressions influences the transfer and penetration of ink in offset printing, for example. In the printing nip, sheet porosity and surface roughness are generally smaller than outside the nip. Paper compression in the printing nip is predominantly reversible. However, depending on the compressibility of paper, significant spatial variation may occur in the compression of thick and thin areas. This leads to nonuniform print. Understanding of the reversible compression behavior of paper is important when improving print uniformity.

The role of furnish composition and sheet structure on the compression behavior of paper has not been systematically studied. For example, one expects intuitively that sheets of high porosity (low density) compress more than sheets of low porosity (high density). However, the quantitative effect of porosity vs. surface roughness is not known. In our study, we wanted to analyze systematic differences in the compression behavior of different papermaking furnishes. In order to obtain reproducible results we concentrated on the reversible pressure-compression behavior. For this purpose we subjected all the samples to a number of compression cycles before the actual compression measurements. As we will show below, this approach leads to systematic effects that can be analyzed with a simple physical model.

EXPERIMENTAL

Sample material

We used a few sets of handsheets whose grammage and density are in Table 1. More details are available in Reference [4]. One of the primary motivations for the different sample sets was the variation of porosity. Sheet porosity is bound to vary in the mixtures of flexible pine kraft fibers and stiff viscose fibers or the long fiber fraction of TMP. The two stiff fibers differ in the fiber cross-section. Viscose fibers are solid while TMP fibers have a collapsable lumen. In addition, we also had mixtures with "porous" pine kraft pulp. After mild alkaline cooking, the pulp had been given a three-stage peroxy-formic acid treatment and a second alkaline cooking. Finally, the pulp was bleached by two-stage peroxide bleaching. Based on the porosity of the fiber wall, these fibers can be assumed to compress easily.

Table 1 Definition of the sample sets

Sample set	Grammage, g/m^2	Density, kg/m^3	Number of test points
Grammage set, pine kraft pulp	8–90	280–710	10
Mixtures of pine kraft and viscose	65–69	270–600	5
Mixtures of pine kraft and TMP long fibers	64	360–610	5
Mixtures of pine kraft and "porous" pulp	90	600–710	3
Birch pulps of different ionic content	63–66	630–680	3
TMP pulps with different fines content	63–65	420–510	5
Pine kraft pulp with 0–45% talc filler	73–80	570–680	5

We also had a few birch kraft pulps of different ionic content to compare with the pine kraft. The ionic form affects the swelling of the fiber and thereby the paper density. These samples were used in order to determine whether pine and birch fiber show different compression behavior. The effect of mechanical pulp fines and the use of filler were illustrated by a separate sample series for each. We expected that the fines are softer than fiber wall and that filler particles would not compress at all. The density of fiber network for the filler containing sheets can be estimated using the assumption that the filler only increases the sheet mass, not its volume. This is reasonable because the filler was talc that has a flat particle shape. This approximation was not, however, used in the experiments.

The pore structure of paper depends on grammage. At low grammages, no pores exist between fibers in the thickness direction of paper. Any compression of a thin sheet should therefore involve a compression of fiber walls and collapse of lumens. However, the situation is a little more complicated because of the high levels of surface roughness may persist at low grammages, no matter how hard one presses the sheet surface. In a rough sheet the compressive force acts on a small fraction of the surface, leading to higher compression than in a sheet with smooth surface and equal porosity.

The sheets containing filler were dried in a drum which leaves both sides of the sheet rough. All other samples were dried on a plate which makes the side dried against a plate glossy.

Removal of the irreversible compressibility

When compressed for the first time, the thickness of paper usually decreases irreversibly and the surfaces smoothen. Additional compression cause only moderate increase in the irreversible compression. Figure 1 shows the result for a series of compression cycles of a copy paper. One can see that after the

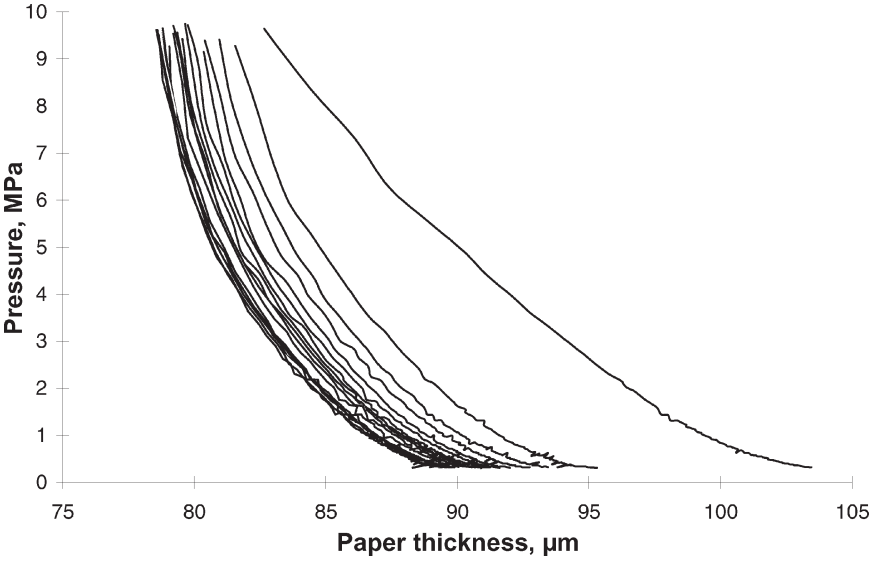

Figure 1 Systematic decrease in the thickness of a copy paper in 20 successive compression cycles. The curves move to the left with increasing number of cycles. Only the part for increasing pressure is shown.

first compression cycle, the shape of the pressure-compression curve remained almost constant. However, the irreversible compression component grew for yet a few cycles.

In our study, we were only interested in the reversible compression behavior. Five compression cycles before the actual measurement are enough to give a good estimate of the completely reversible component of the pressure-compression curve (Figure 1). The pressure-compression curves given below are thus from the sixth compression cycle.

Compression tests

In the compression tests we used a slow pneumatic system with a pressing area of 55 mm × 55 mm. The pressure increase was nonlinear with the rate of increase accelerating towards the end. The maximum pressure, 10 MPa on the paper specimen, was achieved in 90 seconds. Only one sheet at a time was pressed in the current tests. The compression was somewhat nonuniform spatially because of distortions in the device. From thickness measurements after pressing we estimated that the edges of a typical specimen compressed 5–10% (or several micrometers) more than the center.

Two digital sensors measured the separation of the plates with a 0.12-μm resolution. We used the average of these readings. When calculating the compression of paper, we used as a reference thickness the plate separation at 1.0 MPa pressure. In other words, paper compression was not calculated against the standard thickness of paper. We chose this convention because the initial part of the compression curve (at pressures below a few hundred kPa) is often very irregular and shows a lot of variability between specimens. The irregularity arises probably from formation and surface roughness effects that were not of interest to us. The use of the reference thickness at 1 MPa removes practically all the variability between individual specimens.

We measured paper thickness (SCAN-P 7:96) before the experiments and after the sixth compression cycle. The measurements lasted for at most ten minutes after the pressing had ended. The compression tests and thickness measurements were conducted at the standard 50% RH and 23°C. Six parallel samples were compressed for each trial point. Before testing the samples were conditioned according to SCAN-P 2:75.

Porosity

Porosity is the volume fraction of pores in the sheet. Paper compressibility should be sensitive to porosity. In this study, we measured porosity using oil absorption. Oil is absorbed into the sheet and by using the densities of the

sheet and oil we can calculate the porosity of the sheet (Appendix). We used the apparent density of the sheet in the calculation. We tested the method using normal copy paper and found it reasonably well repeatable. A small comparison of the oil absorption method with a porosity measurement from cross-sectional images indicated agreement to within 0.090 absolute units (20 in %-units) for handsheets of porosities ranging from 0.37 to 0.59 [4].

We tried the porosity measurements both before and after the six compression cycles. However, the latter measurement gave unreasonable values, often exceeding the porosity measured before the compression test. The penetration of oil seems to cause some relaxation of the induced, otherwise irreversible compression. Thus we decided not to use the porosity values measured after the compression test. The same problem may naturally also distort the values measured before the compression test.

In principle, sheet porosity (ϕ) can also be estimated from sheet density (ρ_{paper}), if the fiber density (ρ_{fiber}) is known:

$$\phi = 1 - \frac{\rho_{\text{paper}}}{\rho_{\text{fiber}}}. \tag{1}$$

In practice, difficulties arise from the estimation of fiber density and the choice of the proper paper density (apparent vs. effective density). Figure 2 compares apparent density and the porosity measured with oil absorption.

Except for the grammage series, there is a reasonable overall agreement with equation 1 if we use the value of fiber density $\rho_{\text{fiber}} = 1000$ kg/m^3 (Figure 2). We chose this density value because the oil used in the absorption method presumably does not penetrate into the fiber wall. We account for the open lumina and cell wall pores by using fiber density of 1000 kg/m^3 instead of 1500 kg/m^3. The largest differences between the calculated and measured values are 0.1 absolute units or 10%-units. In the filler series, the value of ρ_{fiber} should in principle have included the higher density of the filler material but we did not make this correction.

In the grammage series the measured porosity did not vary significantly but apparent density decreased with decreasing grammage (Figure 2). Analysis of the data in the Appendix shows that sheet thickness and grammage are linearly related, suggesting that the effective density was constant in the grammage series and could have agreed with the measured porosity. Unfortunately, we did not have a direct measurement of effective density available to check if it would give better estimates for porosity than that given by the apparent density.

We conclude that, except for the grammage series, equation 1 gives a reasonable estimate for porosity. In the lack of anything better, we used the

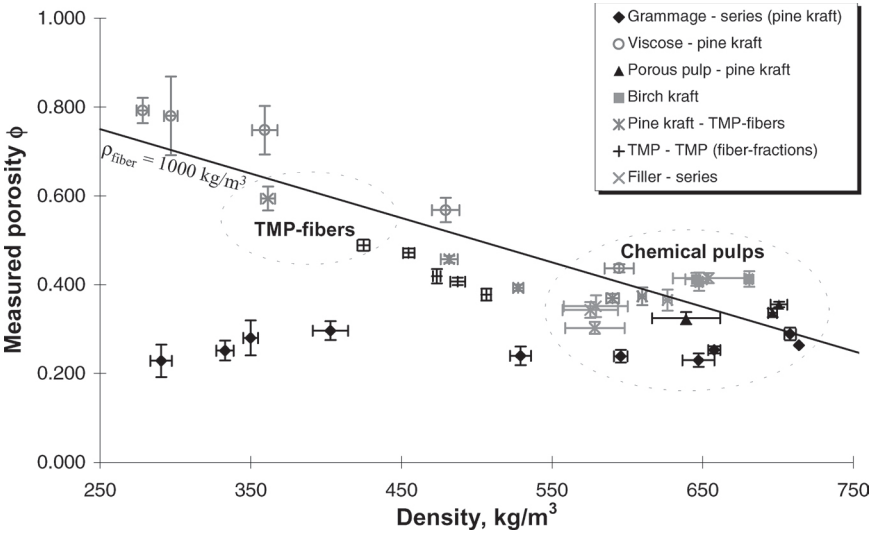

Figure 2 Porosity (before any compressions) against apparent density. Porosity was measured by oil absorption. The line shows porosity calculated from equation 1 using fiber density 1000 kg/m^3. The 95% confidence intervals are given.

density measured after the compression tests as the measure of the porosity that the paper specimens had when we measured the reversible pressure-compression curves. The apparent density values measured after the testing are also given in the Appendix.

MODEL FOR REVERSIBLE COMPRESSION

Several mathematical formulae have been published for the z-directional [2,5–8] and in-plane [9] compression of paper. They provide convenient parametrization to measured pressure-compression curves but no insight to the role of paper structure. For example, Pfeiffer [5] used the following expression for the compression of paper during reeling:

$$p = -K_1 + K_1 \cdot \exp(K_2 \cdot \varepsilon). \tag{2}$$

The model by Salikis and Kuskowski [9] was originally used for the

in-plane compression but the following format is also useful for z-directional compression:

$$\varepsilon = \frac{p}{E_e \cdot (1 - c \cdot p)}. \tag{3}$$

In these equations p is the compression pressure, ε the compressive strain and the other symbols are adjustable parameters.

We fitted these equations to our data using all parameters of the equation as free parameters. The squared error was weighted with the square of compression pressures because our system gives many more data points at low pressures than at high. Figure 3 illustrates the good agreement of equations 2 and 3 with the measured compression curve. Figure 3 also shows another model that we will describe next. It does not agree with the measurement quite as well as the other two expressions.

In order to model the microscopic compression mechanism of the fiber network we assume that only pores between fibers can compress. Two extreme

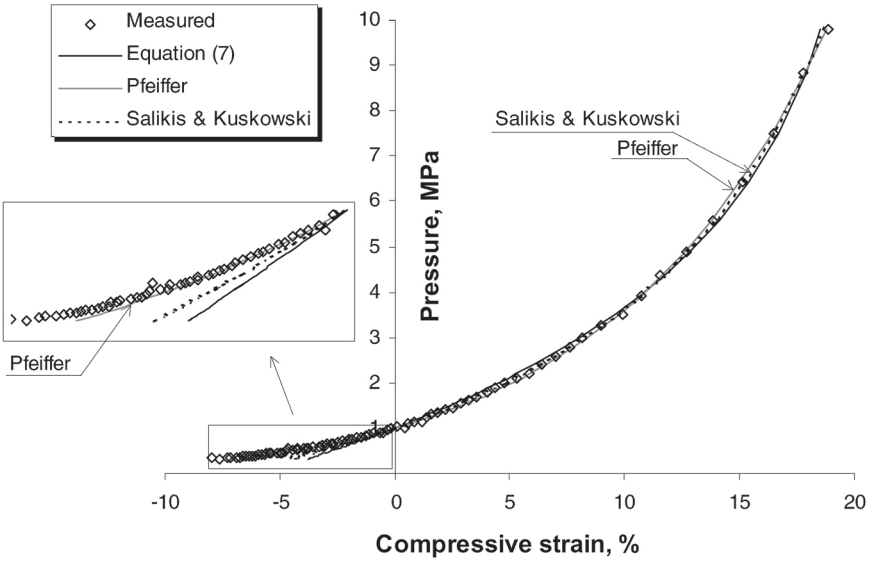

Figure 3 Fitting of equations 2, 3 and 7 to a measured pressure-compression curve at the sixth compression cycle.

cases can be readily considered. In the first case the relative compression of pores (in percents) is constant. In the second case all pores compress by equal amount in absolute units (say, in micrometers).

Consider the first alternative first. The pores then correspond to compressible medium of constant elastic modulus. The pressure-compression curve of the sheet is then determined by the pressure-compression curve of a typical pore. The simplest case would be one of a linear pressure-compression curve of a single pore up to the point where the pore is completely closed. This would happen at 100% compression of the pore. The linear behavior is clearly inconsistent with experimental data (see Figure 3).

On the other hand, at large strains (such as those encountered in compression), it is better to use logarithmic strain instead of the ordinary engineering strain. Whereas the engineering strain is defined as

$$\varepsilon = -\frac{t_2 - t_1}{t_1}, \tag{4}$$

the logarithmic strain is defined as:

$$\varepsilon_{\ln} = -\ln\left(\frac{t_2}{t_1}\right) = -\ln(1 - \varepsilon) \tag{5}$$

where t_1 and t_2 are thicknesses before and after compression. The sign convention gives positive values for compressive strain. When the compression is small, equations 4 and 5 give similar results. The maximum value of ε is 1 (or 100%) but $\varepsilon_{\ln}$ has no upper limit.

In the simplest case the logarithmic strain is linear function of pressure. When substituted in equation 5, this gives for the compression of pores in paper

$$\varepsilon_{\text{pores}} = \left[1 - \exp\left(-\frac{p}{E^*}\right)\right] \tag{6}$$

Here E^* is an elastic modulus characterizing the compression of pores. Finally, we remember the original assumption that only pores compress. When the compressible fraction of sheet thickness is denoted by ϕ^*, we obtain:

$$\varepsilon = \phi^* \cdot \left[1 - \exp\left(-\frac{p}{E^*}\right)\right] \tag{7}$$

This equation fits reasonably well with the experimental results in Figure 3. The deviation is largest at low pressures.

The second alternative is one where all pores compress by the same absolute value (the same amount in micrometers). Physically this case corresponds to all the pores having equal spring constant. The shallowest pores close first and the deepest ones last. We assume that at any point in the sheet there are on the average N pores in the thickness direction of the sheet. The compression of the sheet, Δt, is thus given by

$$\Delta t = N\int_0^y g(h)\cdot h\cdot dh + N\int_y^\infty g(h)\cdot y\cdot dh. \tag{8}$$

where $g(h)$ is the probability distribution of a pore space of height h. The first term describes the pores that have already closed and the second term the pores that are still open. All pores of the latter type have compressed by an equal amount, y.

To a reasonable accuracy, the height distribution of the pore space, g, is exponential [10]:

$$g(h) \approx \frac{1}{\langle h\rangle}\exp\left(\frac{-h}{\langle h\rangle}\right), \tag{9}$$

where $\langle h\rangle$ is the average height of pore space. Substitution to equation 8 gives:

$$\Delta t = N\langle h\rangle\cdot\left[1-\exp\left(\frac{-y}{\langle h\rangle}\right)\right]. \tag{10}$$

The ratio $y/\langle h\rangle$ is the compression of a pore (if the pore is still open) relative to the average height of the pore space. Let it be a linear function of pressure or:

$$\frac{y}{\langle h\rangle} = \frac{p}{E^*} \tag{11}$$

Next observe that $N\langle h\rangle/t$ is sheet porosity, or in the previous notation, $N\langle h\rangle/t = \phi^*$. When we substitute this relationship and equation 11 in equation 10, we obtain again equation 7. We have thus two alternative derivations for equation 7. The latter derivation shows many reasons why the compression curve could be much more complex. In addition to the simplifications

presented by equations 9 and 11, we assumed that all individual pores can be modeled by springs that have a constant value of the spring constant, irrespective of the pore height. Nevertheless, the good agreement between equation 7 and the measurements suggests that the model captures the essential features of the compression of the fiber network structure.

EXPERIMENTAL RESULTS

We measured the reversible pressure-compression curves after five precompression cycles and fitted them to the model, equation 7. Both the parameter ϕ^* and E^* were fitted as free parameters. In the following we will first discuss the compression behavior of the different paper samples and then compare it with paper porosity and furnish composition.

Influence of grammage

The compressive strain of paper decreases with increasing grammage, as shown in Figure 4. This result conforms to previous studies [11,12]. At the lowest grammages the compressive strain does not develop systematically when grammage decreases. This is probably due to the irregular formation of the sheets and the higher compression of the edges of the specimens. Unlike the compressive strain, the absolute compression (thickness reduction in micrometers at any given pressure) decreases systematically when grammage decreases.

With the thinnest sheets, the compression curves turn vertical at pressures from 5–7 MPa. Presumably all pores inside the sheet have collapsed at this point and any further compression would require the compression of fiber wall material.

We fitted the curves from Figure 4 into the model equation 7 using first porosity ϕ^* and elastic modulus E^* as the free variables. The vertical sections of the curves for low grammages were excluded from the curve fitting. The fitting resulted in an elastic modulus growing linearly when grammage grows (Figure 5). The porosity, on the other hand, first decreases and then levels off at $\phi^* = 0.13$ when grammage exceeds 50 g/m^2. The increase in the elastic modulus and the decrease in porosity both contribute to a decrease in compression.

The steady growth of E^* and decrease of ϕ^* with increasing grammage is somewhat surprising. The porosity measured with oil absorption first increases monotonically from 0.23 to 0.30 when grammage grows from 8 to 16 g/m^2, which then fluctuates between 0.23 and 0.29 at higher grammages (see

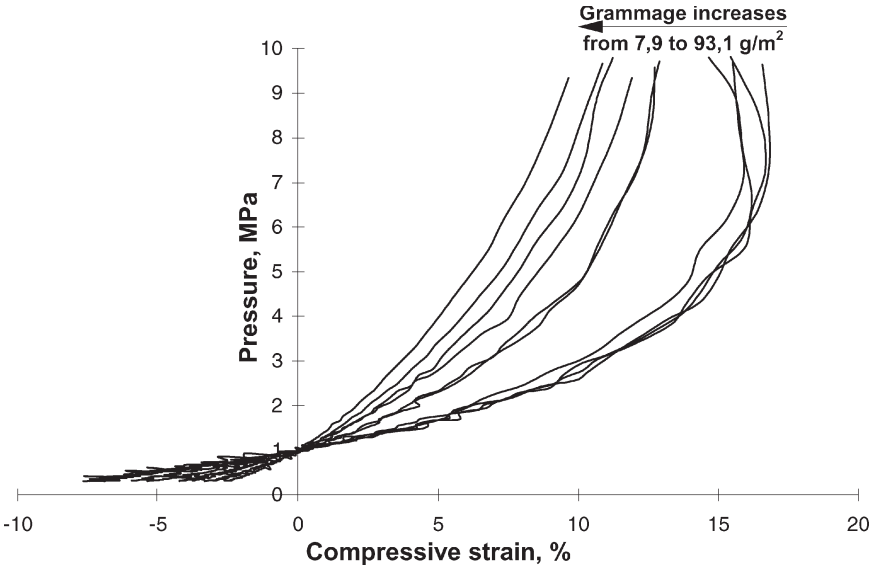

Figure 4 Compression of pine kraft handsheets of different grammage in the sixth compression cycle.

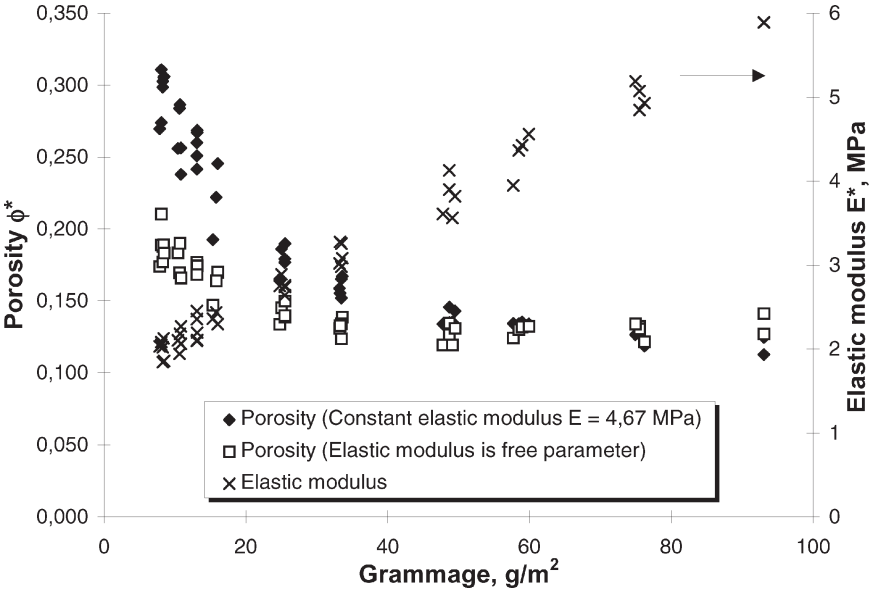

Figure 5 The porosity ϕ^* of the model equation 7 as a function of grammage in handsheets of pine kraft. In the first fit (open squares), the elastic modulus E^* was also a free parameter, the fitted values shown by the crosses. In the second fit (black diamonds), the elastic modulus was constant at $E^* = 4{,}67$ MPa.

the Appendix or Figure 2). The variation in E^* and ϕ^* at the lowest grammages can arise from the proportionately high roughness and large number of holes in the thinnest sheets. Then only a small part of the sheet area carries the applied load, explaining the high compressive strain at the lowest grammages. However, the effect must disappear already at fairly low grammages and therefore the growth of E^* up to the highest grammages cannot be reasoned from sheet structure.

Below we will demonstrate that in the other samples the elastic modulus E^* varied only a little, between 4–5 MPa. A similar value of E^* would seem reasonable also in the grammage series, especially at the higher grammages. Therefore we made a second curve fitting, keeping the elastic modulus constant at $E^* = 4.67$ MPa and allowing only the porosity ϕ^* to change. The value of E^* is the mean value for all the other samples, excluding grammage series. The resulting porosity ϕ^* differs from the first one mainly at low grammages (Figure 5). As Figure 6 shows, the second fitting procedure does not agree with the measured compression curve as well as the procedure where E^* and ϕ^* are free parameters. Although the mathematical form of equation 7 may suggest otherwise, the two parameters E^* and ϕ^* cannot fully

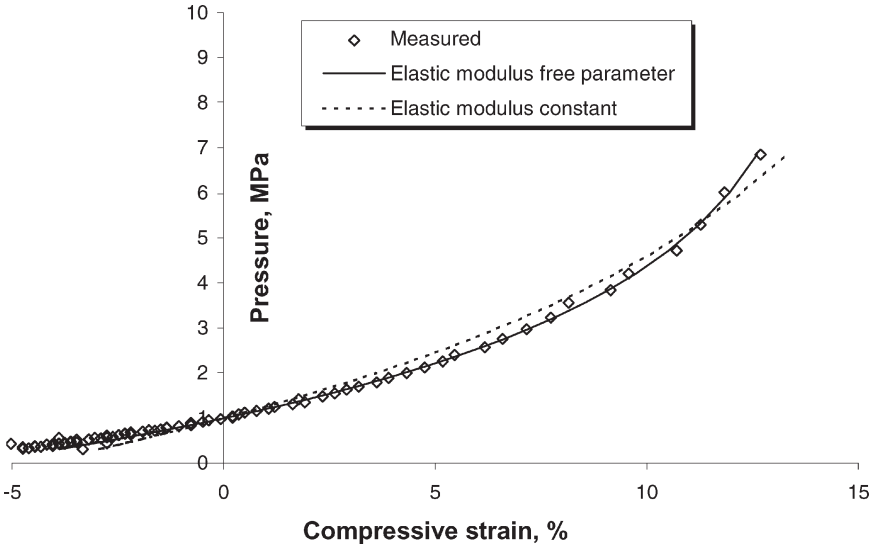

Figure 6 Fitting of equation 7 to a measured pressure-compression curve at the sixth compression cycle when elastic modulus is a free parameter (dashed curve) and constant $E^* = 4.67$ MPa (solid curve). Grammage of the sheet 25 g/m^2.

compensate for one another. This gives added credibility to the fitted parameter values.

Influence of fiber composition

When we added mechanical pulp to chemical pulp, even in small amounts, the reversible compression increased significantly (Figure 7). The increase can be seen clearly in the fitted model parameters as an increase in porosity ϕ^* and a decrease in elastic modulus E^* (Figure 8). The result is reasonable because mechanical pulp gives paper higher porosity than chemical pulp.

The mechanical pulp fines fraction has a surprisingly small effect on the sheet compression that decreases only slightly when the fines content increases. This is reflected in the corresponding small increase in E^* and the small decrease in ϕ^* (Figure 9). The porosity measured by oil absorption decreases with increasing fines content much more than ϕ^* (Figure 2).

The effect of filler gives an interesting comparison for the effect of fines. At first the filler addition increases sheet compression at a given pressure, but at higher filler contents compression becomes constant. The fitted value of the porosity ϕ^* again remains almost constant (Figure 10), in a similar manner as

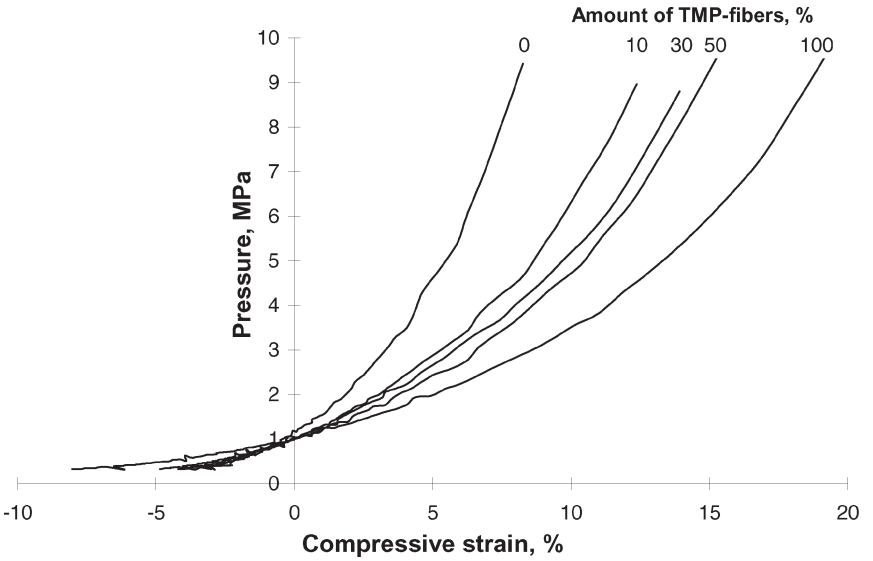

Figure 7 Compression curves for handsheets containing a mixture of TMP long fibers and pine kraft pulp.

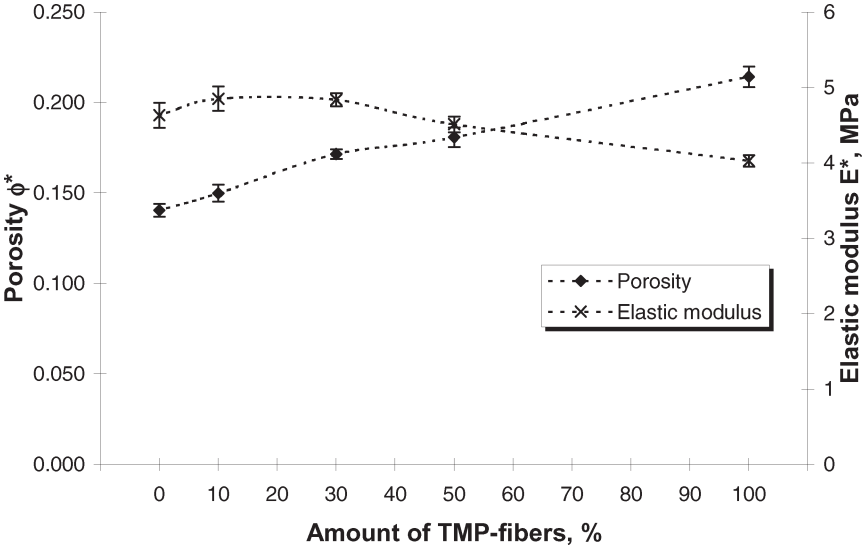

Figure 8 The parameters of the model equation 7 fitted for handsheets containing TMP fibers and pine kraft pulp.

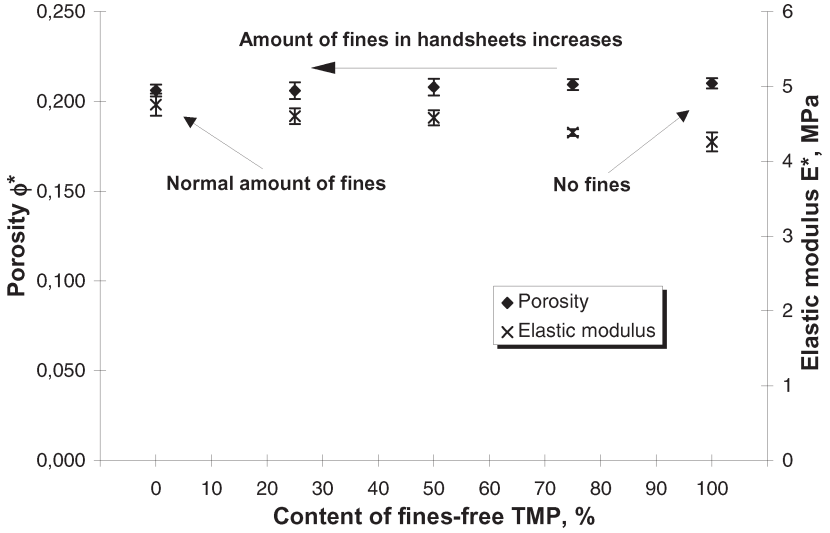

Figure 9 The parameters of model 7 for handsheets containing different mixtures of whole TMP pulp and the fiber fractions of the same pulp. Fines content decreases from the normal level to zero as the whole pulp is replaced with the fibers.

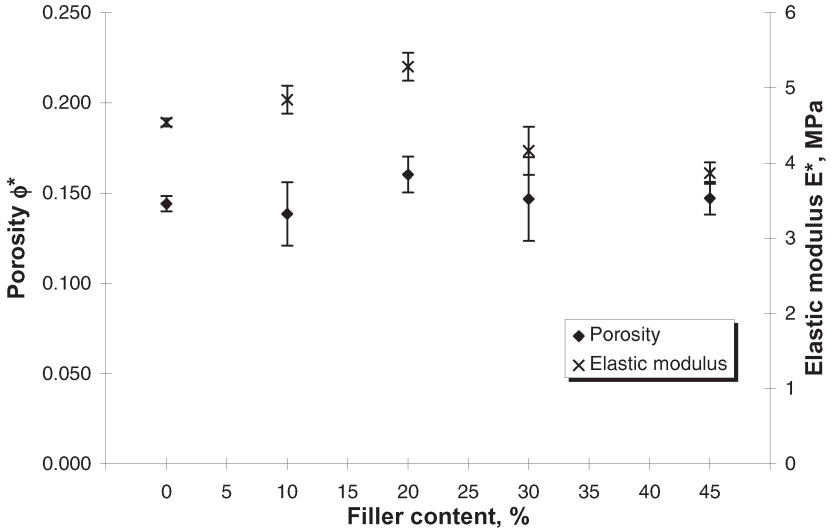

Figure 10 The parameters of model 7 for pine kraft handsheets containing different amounts of talc filler.

with the fines addition. The elastic modulus E^* first increases and then decreases with increasing filler content. This irregular behavior is probably due to the unusually poor formation of the sheets with high filler content.

Coupling between model parameters and paper properties

Of the model parameter values obtained by fitting to the pressure-compression curves, the model elastic modulus, E^*, varies only a little in all our samples whereas the model porosity, ϕ^*, varies significantly more. This makes sense because we expect that ϕ^* is related to the porosity of paper while E^* could be determined by the fiber properties.

We should then compare the model porosity ϕ^* with a porosity of paper measured after the six compression cycles. Porosity should not change in the sixth cycle because the compression behavior is almost completely reversible. Unfortunately we did not succeed in measuring this porosity with the oil absorption method. The second best alternative is to use sheet density (after the six compression cycles) as the measure of porosity.

Figure 11 shows that the density measured after the six compression cycles has a reasonable relationship to the model porosity ϕ^*. Sheet porosity decreases linearly with increasing density (equation 1). According to Figure 2,

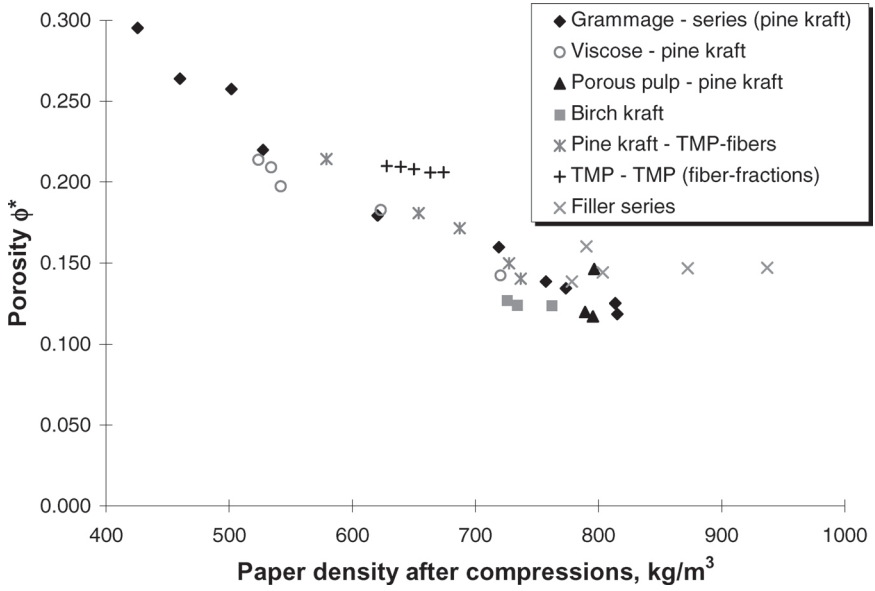

Figure 11 The porosity ϕ^* of model 7 against the original value of apparent density measured before any compressions.

there is little difference between different paper compositions in the density-porosity relationship. There are three major deviations from the general trend, the sheets with low grammage (at most 15 g/m^2), the sheets with different mechanical pulp fines contents and the sheets with high filler content.

The data for the grammage series comes from the second curve fitting where the elastic modulus E^* was held constant. As we already discussed, the relatively high values of the model porosity ϕ^* at low grammages probably arises from the roughness and holes in these sheets. In the series with different fines contents, we can force the values of ϕ^* down to the general trendline by setting $E^* = 4$ MPa when fitting the model equation 7 to the measured pressure-compression curves.

At the high filler contents (30% and 45%), paper density gives an underestimate for sheet porosity because of the high density of the filler material. Assuming that the filler occupies no space at all, the equivalent density could be as low as 520 kg/m^3 for the sheets with 45% filler content. The proper density value to estimate the true porosity in this case is probably somewhere between 520 and 940 kg/m^3, perhaps at ca. 700 kg/m^3 implied by the model fit.

The model elastic modulus E^* varies a little with the density measured after the compression tests (Figure 12). This variation could arise from the furnish composition but we cannot be sure of this. It would be physically sensible that the value of the elastic modulus would be independent of sheet porosity whose effect is already accounted for in the porosity parameter ϕ^*.

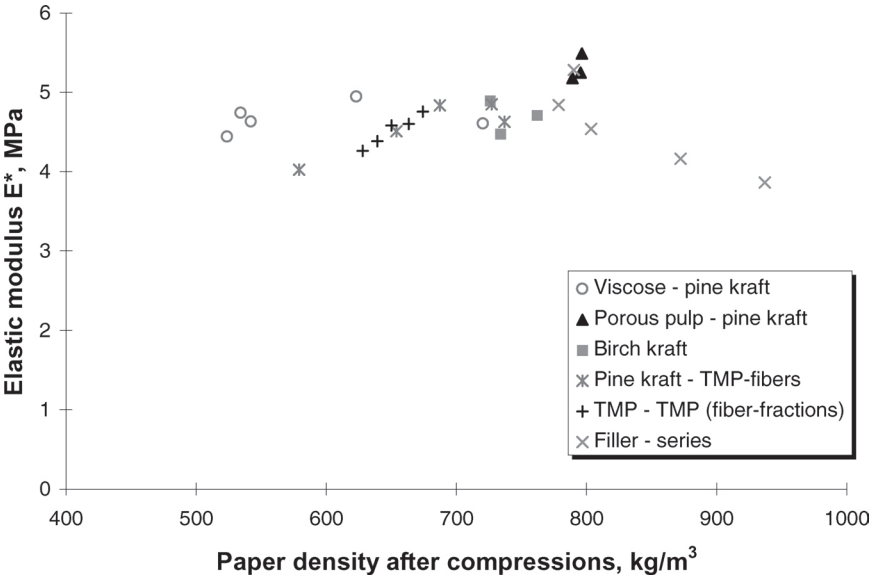

Figure 12 The elastic modulus of model 7 against the original value of apparent density measured before any compressions.

DISCUSSION

We have studied the reversible component of paper compression, revealed by a few compression cycles before the actual measurement. The measured pressure-compression curves agree reasonably well with the simple model equation 7. The model has a simple relationship to the structure of paper and thus it is applicable to the study of the compression behavior of the fiber network.

The porosity of paper mainly affects the porosity parameter ϕ^*. In most cases the fitted values of ϕ^* change from 0.13 to 0.22 when paper density

decreases from 800 to 500 kg/m^3. Indirect evidence, using data measured before the compression tests (Figure 2), suggests that the corresponding sheet porosity is higher, ranging from 0.2 to 0.5. The values of ϕ^* are thus physically sensible because the fiber network is bound to have pores that are so closely surrounded by fibers that the compression of the pore would necessarily require a compression of the surrounding fiber walls. A more detailed comparison of sheet porosity and the volume fraction ϕ^* is not warranted because we did not have available a direct porosity measurement for the samples that had undergone the five compression cycles before the actual measurement.

We believe that the use of apparent density as an indicator of sheet porosity explains why some samples deviate from the general trend in Figure 11. Especially in the sheets of low grammage and those of high filler content, sheet porosity cannot be calculated from apparent density using equation 1.

The effective elastic modulus of the model ranges from $E^* = 4$ to 5 MPa. The relative variability in E^* is clearly smaller than in ϕ^*. The lower values seem to apply to mechanical pulp and the higher to chemical pulp but this can be an artifact caused by the fitting procedure. If we use ϕ^* as the only free parameter, the value of E^* can be fixed to a constant value of ca. 4.5 MPa without a significant loss of agreement between the model and measured pressure-compression curves. Thus it is impossible to know if E^* really depends on the furnish composition. Even if it did, the effects of fiber type, fines and filler are surprisingly small considering the measured variations in E^*. It seems that paper porosity is the primary factor controlling the reversible compressibility of paper.

The key element in our experiments was the removal of the irreversible component of compression. We achieved this by a series of compression cycles applied before the actual measurements. The irreversible compression caused by this sample preparation is presumably sensitive to the original surface roughness, but this effect is beyond the scope of our study.

REFERENCES

1. Ivarsson, B.W., "Compression of cellulose fiber sheets", *Tappi* **39**(2): 97–104 (1956).
2. Schaffrath, H.-J. and Göttsching, L., "The behaviour of paper under compression in z-direction", *1991 International Paper Physics Conference*: Kona, Hawaii, 22–26 September 1991. TAPPI Press, Atlanta, USA: Book 2, 489–510 (1991).
3. Schaffrath H.-J. and Göttsching, L., Das Kompressionsverhalten von Papier in z-Richtung: *Papier* **46**(10A), V74–V81 (1992).

4. Kananen, J., *Paperin rakenteen vaikutus kokoonpuristuvuuteen*. Master's Thesis, Helsinki University of Technology, Laboratory of Paper Technology, 132 p (1999).
5. Pfeiffer, J.D., Surface winding to overcome the strain deficiency: *Tappi J.* **73**(10), 247–250 (1990).
6. Rodal, J., Soft-nip calendering of paper and paperboard: *Tappi J*. **90**(5), 177–186 (1989).
7. Ellis, E.R., Jewett, K.B., Ceckler, W.H. and Thompson, E.V., Dynamic Compression of Paper III. Compression Equation for Cellulose Mats. *1982 Annual Meeting: American Institute of Chemical Engineers*. Los Angeles, CA: November (1982).
8. Valentin, F.B., Modeling paper strain in a calender nip: *Tappi J.* **82**(8), 183–188 (1999).
9. Salikis, P. and Kuskowski, S.J., Constitutive modeling of paper accounting for rate of load and transient relative humidity effects: *Tappi J.* **81**(2), 181–188 (1998).
10. For experimental demonstration of the exponential distribution, see e.g. K. Niskanen, N. Nilsen, E. Hellén, Mikko Alava: KCL-PAKKA: Simulation of the 3D structure of paper: in *The Fundamentals of Papermaking Materials: The Eleventh Fundamental Research Symposium*. Pira International, Sep 21–26, Cambridge: 1273–1291 (1997).
11. Jackson, M. and Ekström, L., Studies concerning the compressibility of paper: *Svensk Papperstidn*. **67**(29), 807–821 (1964).
12. Yamauchi, T., Compressibility of Paper Measured by Using a Rubber Platen Thickness Gauge. *Appita J.* **42**(3), 222–224 (1989).

APPENDIX

Table A1. The parameters (ϕ^*, E^*) of the model 7, apparent density and porosity of handsheets for grammage series. Porosity is measured by oil absorption. 95% confidence intervals (CI) are given in the table.

Grammage, g/m^2	Porosity ϕ^*		Elastic modulus E^*, MPa		Measured density (before and after compressions, kg/m^3)		Measured porosity ϕ	
	AVG	CI	AVG	CI	before	after	AVG	CI
8,2	0,187	0,009	2,00	0,08	291	425	0,228	0,037
10,7	0,175	0,010	2,11	0,11	333	460	0,252	0,022
13,1	0,174	0,003	2,24	0,14	350	502	0,280	0,039
15,7	0,160	0,004	2,36	0,18	403	527	0,296	0,051
25,2	0,141	0,055	2,75	0,08	529	621	0,240	0,021
33,4	0,132	0,005	3,12	0,12	596	719	0,239	0,014
48,8	0,126	0,006	3,80	0,20	647	757	0,230	0,015
58,7	0,130	0,003	4,33	0,20	658	773	0,253	0,008
75,5	0,130	0,005	5,01	0,15	708	814	0,289	0,015
93,1	0,134	0,014	5,89	0,01	714	815	0,264	–

Table A2 The parameters (ϕ^*, E^*) of the model 7, apparent density and porosity of handsheets for porous-pulp- series. Porosity is measured by oil absorption. 95% confidence intervals (CI) are given in the table.

Amount of porous pulp, %	Porosity ϕ^*		Elastic modulus E^*, MPa		Measured density (before and after compressions, kg/m^3)		Measured porosity ϕ	
	AVG	CI	AVG	CI	before	after	AVG	CI
0	0,146	0,013	5,49	0,51	639	796	0,324	0,014
50	0,117	0,004	5,25	0,24	696	795	0,337	0,009
100	0,120	0,009	5,18	0,12	701	789	0,355	0,006

Table A3 The parameters (ϕ*, E*) of the model 7, apparent density and porosity of handsheets for viscose series. Porosity is measured by oil absorption. 95% confidence intervals (CI) are given in the table.

Amount of viscose, %	Porosity ϕ*		Elastic modulus E*, MPa		Measured density (before and after compressions, kg/m^3)		Measured porosity ϕ	
	AVG	CI	AVG	CI	before	after	AVG	CI
0	0,142	0,007	4,60	0,11	595	720	0,437	0,009
25	0,183	0,009	4,94	0,19	479	623	0,568	0,028
50	0,197	0,002	4,63	0,08	359	542	0,748	0,055
60	0,209	0,006	4,74	0,16	297	534	0,780	0,088
70	0,214	0,012	4,44	0,27	278	524	0,792	0,029

Table A4 The parameters (ϕ*, E*) of the model 7, apparent density and porosity of handsheets for TMP-pine kraft series. Porosity is measured by oil absorption. 95% confidence intervals (CI) are given in the table.

Amount of TMP, %	Porosity ϕ*		Elastic modulus E*, MPa		Measured density (before and after compressions, kg/m^3)		Measured porosity ϕ	
	AVG	CI	AVG	CI	before	after	AVG	CI
0	0,140	0,004	4,63	0,16	610	737	0,374	0,021
10	0,150	0,005	4,85	0,16	590	727	0,369	0,010
30	0,171	0,003	4,83	0,09	528	687	0,393	0,007
50	0,181	0,005	4,51	0,11	482	654	0,457	0,008
100	0,214	0,006	4,03	0,08	361	579	0,594	0,028

Table A5 The parameters (ϕ^*, E^*) of the model 7, apparent density and porosity of handsheets for birch kraft series. Porosity is measured by oil absorption. 95% confidence intervals (CI) are given in the table.

Ions of acid groups	Porosity ϕ^*		Elastic modulus E^*, MPa		Measured density (before and after compressions, kg/m^3)		Measured porosity ϕ	
	AVG	CI	AVG	CI	before	after	AVG	CI
Al	0,124	0,003	4,48	0,16	646	734	0,412	0,015
Ca	0,127	0,003	4,89	0,18	647	726	0,406	0,021
H	0,124	0,002	4,71	0,14	681	762	0,413	0,018

Table A6 The parameters (ϕ^*, E^*) of the model 7, apparent density and porosity of handsheets for TMP-series. Porosity is measured by oil absorption. 95% confidence intervals (CI) are given in the table.

Amount of long- fiber fraction, %	Porosity ϕ^*		Elastic modulus E^*, MPa		Measured density (before and after compressions, kg/m^3)		Measured porosity ϕ	
	AVG	CI	AVG	CI	before	after	AVG	CI
0	0,206	0,003	4,75	0,15	506	674	0,378	0,014
25	0,206	0,005	4,6	0,11	487	663	0,407	0,008
50	0,208	0,005	4,58	0,10	473	650	0,419	0,016
75	0,209	0,003	4,38	0,05	455	639	0,472	0,010
100	0,210	0,003	4,26	0,13	425	628	0,489	0,013

Table A7 The parameters (ϕ*, E*) of the model 7, apparent density and porosity of handsheets for filler series. Porosity is measured by oil absorption. 95% confidence intervals (CI) are given in the table.

Filler content, %	Porosity ϕ*		Elastic modulus E*, MPa		Measured density (before and after compressions, kg/m^3)		Measured porosity ϕ	
	AVG	CI	AVG	CI	before	after	AVG	CI
0	0,144	0,004	4,54	0,054	627	803	0,365	0,024
10	0,138	0,018	4,84	0,184	578	778	0,302	0,014
20	0,160	0,010	5,28	0,186	575	790	0,343	0,018
30	0,147	0,023	4,16	0,320	579	872	0,351	0,025
45	0,147	0,009	3,86	0,142	654	937	0,415	0,012

Transcription of Discussion

REVERSIBLE COMPRESSION OF SHEET STRUCTURE

Juha Kananen, Hanna Rajatora and Kaarlo Niskanen
KCL Science and Consulting

Patrice Mangin Centre Technique du Papier

Can you provide me with your physical explanation of the elastic modulus of a pore? Although I have one in mind I would like to listen to your own explanation. The second is more a comment. I trust that the discrepancy you find with the fillers might simply be due to the pore size distribution which varies with filler addition. It is indeed a very complex phenomenon.

Juha Kananen

The first question about the elastic modulus of the pores – in real life you can't have an elastic modulus of the pores. We assumed that the fibres do not compress. In this case a reasonable explanation for the elastic modulus of our model is that the pores have some kind of apparent elastic modulus. This elastic modulus describes the ability of the fibre network to resist the pressure applied on it.

Tom Browne Paprican

Just a suggestion – you said that the strain at low grammage went vertical with low 5 MPa, I would assume that you've got a lot of areas in the sheet where you have exceeded the density of cellulose locally – that's undoubtedly what is happening. And probably if you could go higher it would start to level off as you compress cellulose.

Juha Kananen

Yes that is true. The compression behaviour of your network depends on the elastic modulus of the fibres after this turning point.

Kit Dodson Department of Mathematics, UMIST

Back to the last slide [Summary – not in preprints]. The second bullet point on porosity you viewed as a problem with your model. I consider it an opportunity to probe some theory because if you make it give the right porosity, then it is perhaps possible to use some of our statistical geometric theories which give you the distribution of porosities even in non-random structures. This may help both to probe the theory and to shed light on the variability of the incompressible pores.

Juha Kananen

Good point. Thank you for your suggestion.

Jean-Claude Roux EFPG

Have you tested different shapes of pressure-increase distribution and were your results invariant or not?

Juha Kananen

We don't have the possibility to use different kinds of pressure increase rates in the device. It is just a simple pump that increases the pressure in the compression cell. The device used in the experiments is a simple compression cell in which the rate of pressure increase is determined by the structure of the device and the properties of the pressure of the device.

Ning Yan University of Toronto

I have a question about the irreversible compression. You seem to attribute that to only overcome the surface roughness. Don't you think that the pore would deform during that first 5 or 6 cycles of your compression? So the porosity obtained through your fitting, it's actually an altered porosity and it's not the original one? Could you clarify that?

Juha Kananen

Naturally the pressure deformed in the pre-compressions. We can see that the porosity given by the model is significantly smaller than the one measured before the compression and your interpretation on the porosity could quite correct. As I said, we didn't have a measurement for the porosity after the

compressions, because the oil absorption method didn't seem to work for those sheets.

Wadood Hamad International Paper

I have a two-fold question. You made a reference to Pfeiffer's equation about the mechanical properties of a stack of sheets of paper, and I have a thought if you were to extend some of the work from a single sheet to a stack of sheets and you have a plot of compressive strain versus stack thickness, or number of layers, would you anticipate to have individual curves – i.e. not one curve for a number of different stack heights – which also means that in some respect would you also anticipate different slopes?

Juha Kananen

Actually we made measurements with a stack of sheets but those aren't reported here. We detected the behaviour you described, the effect of stacking sheets and the influence of grammage is the same.

Wadood Hamad

In other words you do have individual curves if you were to plot compressive strain versus stack height? You don't have one curve, you have a number of curves, is that right? Then that would also be related to the fact that you have different elasticity modulii, which may not be far removed from the fact that you show variations in your elasticity modulii for a single sheet.

Juha Kananen

You are right we should have taken into account the effect of grammage. The values of the elastic modulus of our model would be more in formative if we had subtracted the effect of grammage.